

Colloquium: Unusual resonators: Plasmonics, metamaterials, and random media

Konstantin Y. Bliokh

*Advanced Science Institute, The Institute of Physical and Chemical Research (RIKEN), Wako-shi, Saitama 351-0198, Japan
and Institute of Radio Astronomy, 4 Krasnoznamyonnaya St., Kharkov 61002, Ukraine*

Yury P. Bliokh

*Advanced Science Institute, The Institute of Physical and Chemical Research (RIKEN), Wako-shi, Saitama 351-0198, Japan
and Department of Physics, Technion-Israel Institute of Technology, Haifa 32000, Israel.*

Valentin Freilikher

Department of Physics, Bar-Ilan University, Ramat-Gan 52900, Israel

Sergey Savel'ev

*Advanced Science Institute, The Institute of Physical and Chemical Research (RIKEN), Wako-shi, Saitama 351-0198, Japan
and Department of Physics, Loughborough University, Loughborough LE11 3TU, United Kingdom*

Franco Nori

*Advanced Science Institute, The Institute of Physical and Chemical Research (RIKEN), Wako-shi, Saitama 351-0198, Japan;
Center for Theoretical Physics, Department of Physics, Applied Physics Program, Center for the Study of Complex Systems, The University of Michigan, Ann Arbor, Michigan 48109-1040, USA;
and CREST, Japan Science and Technology Agency (JST), Kawaguchi, Saitama 332-0012, Japan*

(Published 1 October 2008)

Super-resolution, extraordinary transmission, total absorption, and localization of electromagnetic waves are currently attracting growing attention. These phenomena are related to different physical systems and are usually studied within the context of different, sometimes rather sophisticated, approaches. Remarkably, all these seemingly unrelated phenomena owe their origin to the same underlying physical mechanism, namely, wave interaction with an open resonator. Here we show that it is possible to describe all of these effects in a unified way, mapping each system onto a simple resonator model. Such description provides a thorough understanding of the phenomena, explains all the main features of their complex behavior, and enables one to control the system via the resonator parameters: eigenfrequencies, Q factors, and coupling coefficients.

DOI: [10.1103/RevModPhys.80.1201](https://doi.org/10.1103/RevModPhys.80.1201)

PACS number(s): 42.25.Bs, 73.20.Mf, 78.20.-e, 42.25.Dd

CONTENTS

I. Introduction	1201	C. Critical coupling in optics and plasma physics	1207
A. Veselago-Pendry's "perfect lens"	1202	D. Super-resolution of LHM lenses	1208
B. Extraordinary optical transmission	1202	IV. Random Media	1209
C. Total absorption of electromagnetic waves	1202	A. Resonant tunneling	1209
D. Localized states	1203	B. Critical coupling	1210
II. Classical Resonators	1203	V. Concluding Remarks	1210
A. Basic features	1203	Acknowledgments	1211
B. Plane wave interacting with a resonator	1204	References	1211
C. Coupled resonators	1204		
III. Surface Plasmon-Polariton Systems	1205		
A. Basic features	1205		
B. Enhanced transparency of a metal film	1206		

I. INTRODUCTION

Left-handed materials, plasmon-polariton systems, and localized modes in random media are currently attracting the ever-increasing interest of physicists and engineers. This is due to both the fundamental character of

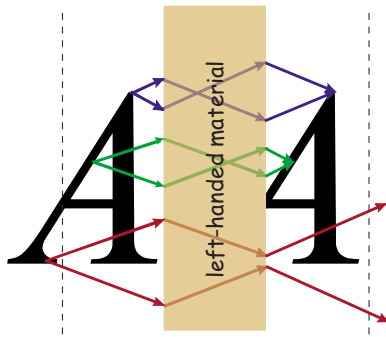


FIG. 1. (Color online) A flat slab of left-handed material can act as a lens forming a perfect 3D image of any object located at a distance less than the slab thickness from the surface.

the problems and promising applications in photonics, subwavelength optics, random lasing, etc. There have been a number of separate investigations and reviews of these phenomena (see, e.g., Lifshits *et al.*, 1988; Sheng, 1990; Freilikher and Gredekskul, 1992; Bliokh and Bliokh, 2004; Smith *et al.*, 2004; Eleftheriades and Balman, 2005; Zayats *et al.*, 2005; Ozbay, 2006; Veselago and Narimanov, 2006; Garcia de Abajo, 2007; Genet and Ebbesen, 2007; Maier, 2007; Shalaev, 2007), but no detailed comparison has been attempted in spite of their deep underlying similarities. Discussing analogies between these systems and with their simple classical counterparts provides a more unified understanding, new insights, and can be illuminating. There are numerous examples of fundamental physical phenomena that can be explained in terms of classical oscillators. Resonators provide the next-step generalization revealing additional common features, such as the critical-coupling effect, crucial for open-wave systems with dissipation. Below, we describe the complex systems mentioned above and analyze them in terms of simple resonator models. Note that here we do not consider microwave and optical resonators, quantum dots, Mie resonances, impurity zones in periodic structures, cavities in photonic crystals, etc. Our goal is to demonstrate that a broad variety of physical phenomena in systems that do *not* contain conventional resonant cavities nonetheless can be adequately described in terms of classical resonators.

A. Veselago-Pendry's "perfect lens"

In 1968, Veselago examined electromagnetic wave propagation in a virtual medium with simultaneous negative permittivity and permeability (Veselago, 1967). He showed that such a left-handed medium (LHM) was characterized by an unusual negative refraction: the incident and refracted beams at the interface between the LHM and ordinary media (hereafter, the vacuum) lie on the same side of the normal to the interface. This property implies that a flat LHM slab can act as a lens forming a three-dimensional (3D) image of the object, as illustrated in Fig. 1. Interest in LHM grew after Pendry's paper (Pendry, 2000), where it was shown that a LHM slab can act as a *perfect* lens. Namely, a LHM slab with

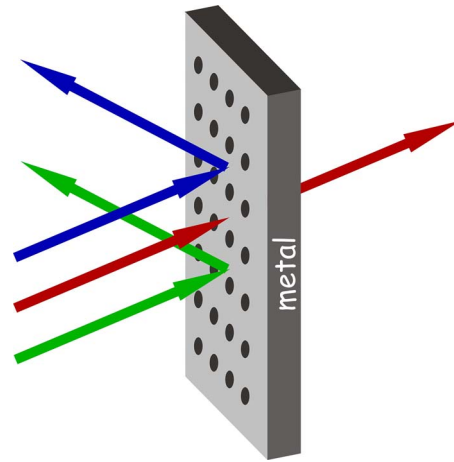


FIG. 2. (Color online) Resonant transparency of a perforated metal film. A periodically modified (perforated or corrugated) optically thick metal film becomes essentially transparent for certain resonant frequencies or angles of incidence.

permittivity and permeability having the same absolute value as in the surrounding medium ($\epsilon = \mu = -1$) forms a perfect copy of an object: all details of the object, even smaller than the wavelength of light, are reproduced (for reviews, see, e.g., Bliokh and Bliokh, 2004; Smith *et al.*, 2004; Eleftheriades and Balman, 2005; Veselago and Narimanov, 2006; Shalaev, 2007). In practice, left-handed materials are artificial periodic structures (metamaterials), and any "perfect lens" will have a finite resolution limited by the size of the unit cell.

B. Extraordinary optical transmission

Metallic thin films can also provide super-resolution for the near-evanescent field (Pendry, 2000; Fang *et al.*, 2005). But for propagating waves, a metallic layer acts as a very good mirror: only an exponentially small part of the radiation can penetrate through it. Surprisingly, Ebbesen *et al.* (1998) found that an optically opaque metal film perforated with a periodic array of subwavelength-sized holes was abnormally *transparent* for certain resonant frequencies or angles of incidence; see Fig. 2. The energy flux through the film can be orders of magnitude larger than the cumulative flux through the holes when considered as isolated (for reviews, see, e.g., Zayats *et al.*, 2005; Garcia de Abajo, 2007; Genet and Ebbesen, 2007). In addition to its fundamental interest, this effect offers applications as tunable filters, spatial and spectral multiplexors, etc. (see, e.g., Sambles, 1998; Lezec *et al.*, 2002).

C. Total absorption of electromagnetic waves

Total internal reflection (TIR) occurs when an oblique light beam strikes an interface between two transparent media, and the refractive index is smaller on the other side of the interface. For instance, the incident light is totally reflected from the prism bottom (which is the TIR surface), as shown in Fig. 3(a). A polished silver

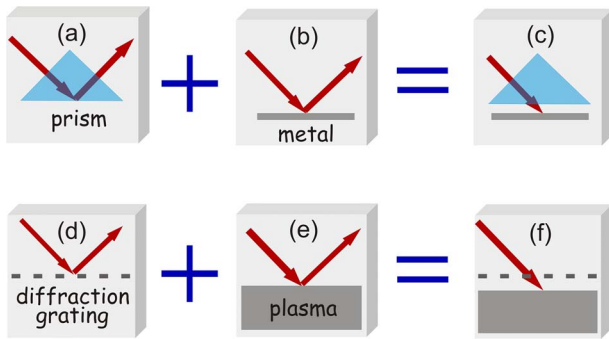


FIG. 3. (Color online) The total absorption of electromagnetic waves in (a)–(c) optics and (d)–(f) plasma physics. Strikingly, even though elements (a), (b) or (d), (e) act separately as very good mirrors, their combination can absorb all the incident radiation (c), (f).

plate is also a good mirror that reflects all incident light, as shown in Fig. 3(b). However, when the TIR surface and the plate are located right next to each other, the reflected beam can disappear and all the light can be *totally absorbed* by the silver plate (Otto, 1968), as shown in Fig. 3(c).

Total absorption can also be observed in the microwave frequency band. When replacing the prism by a reflecting subwavelength diffraction grating, Fig. 3(d), and the silver plate by an overdense plasma [i.e., a plasma whose Langmuir (plasma) frequency is higher than the incident wave frequency], Fig. 3(e), the same effect appears: the incident electromagnetic wave can be totally absorbed by the plasma (Bliokh *et al.*, 2005; Wang *et al.*, 2006), Fig. 3(f), even though both elements act separately as good mirrors.

D. Localized states

Extraordinary optical transmission and total absorption can be observed in a quite different system: 1D random dielectric media. Although the medium is locally transparent, the wave field intensity typically decays exponentially deep into the medium, so that a long enough sample reflects the incident wave as a good mirror. This decay occurs because of multiple wave scattering in randomly inhomogeneous media producing a strong (Anderson) localization of the wave field (Anderson, 1958) (for reviews, see, e.g., Lifshits *et al.*, 1988; Sheng, 1990; Freilikher and Gredeskul, 1992). A simple manifestation of this effect is the almost total reflection of light from a thick stack of transparencies (Berry and Klein, 1997). However, there is a set of resonant frequencies, individual for each random sample, which correspond to a *high transmission* of the wave through the sample accompanied by a large concentration of energy in a finite region inside the sample (Azbel, 1983; Azbel and Soven, 1983) (see Fig. 4). Like optical “speckle patterns,” such resonances (localized states) represent a unique “fingerprint” of each random sample. In active random media, regions that localize waves are sources of electromagnetic radiation producing a so-called random

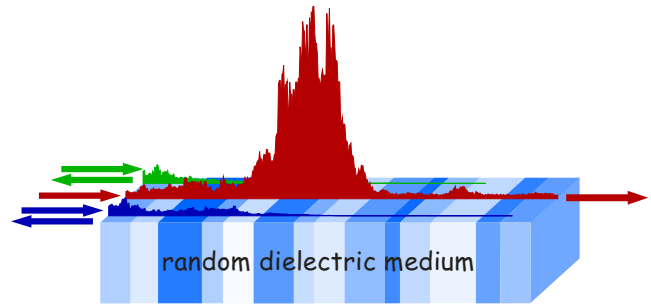


FIG. 4. (Color online) Resonant wave transmission through a 1D random dielectric sample. The spatial distributions of the intensity of the resonant (central) and nonresonant (edge) waves are depicted on the top of the sample, which is displayed schematically.

lasing effect, which offers the smallest lasers, just a few wavelengths in size (Cao *et al.*, 1999; Wiersma, 2000; Milner and Genack, 2005). If the sample has small losses, the resonant transparency can turn into a *total absorption* of the incident wave (Bliokh *et al.*, 2006).

II. CLASSICAL RESONATORS

A. Basic features

The notion of a resonator implies the existence of eigenmodes *localized* in space. The localization of modes is usually achieved by a sandwich-type mirror-cavity-mirror structure, which is analogous to a quantum-mechanical potential well bounded by potential barriers and can be of any nature (see Fig. 5). In a closed resonator without dissipation, each mode is characterized by its resonant frequency (energy level) ω_{res} and spatial structure of the field $\chi(\mathbf{r})$. The eigenmode field Ψ can be factorized as

$$\Psi(\mathbf{r}, t) = \psi(t)\chi(\mathbf{r}),$$

where ψ is a solution of the harmonic-oscillator equation,

$$\frac{d^2\psi}{dt^2} + \omega_{\text{res}}^2\psi = 0.$$

Depending on whether the modes are localized in all spatial dimensions or not, the resulting spectrum can be either discrete or continuous.

The resonator can be nonconservative due to internal *dissipation* of energy. Furthermore, the barriers can allow small energy *leakage* either from or to the cavity, e.g., due to “under-barrier” tunneling via evanescent waves. In such cases, one has to consider the resonator as an open system with quasimodes characterized by fuzzy energy levels of a finite width, Fig. 5. The time dependence of the fields is not purely harmonic anymore and can be described as an oscillator with damping,

$$\frac{d^2\psi}{dt^2} + \omega_{\text{res}}Q^{-1}\frac{d\psi}{dt} + \omega_{\text{res}}^2\psi = 0. \quad (1)$$

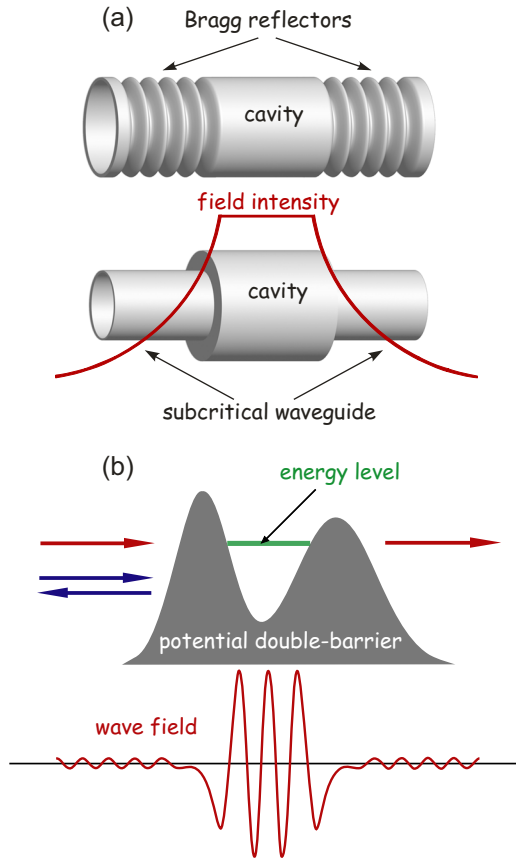


FIG. 5. (Color online) Examples of classical and quantum open quasi-1D resonators. (a) A waveguide segment (cavity) is surrounded by Bragg-reflecting or subcritical segments (acting as barriers). The field inside the resonator can interact with an external wave field through nonpropagating evanescent modes in the barriers. A 3D generalization of the top system can be a cavity inside a photonic crystal in the frequency gap. (b) Any potential well can represent a quantum resonator. Open resonators are surrounded by finite-width barriers. An incident particle can effectively tunnel through both energy barriers when its energy coincides with one of the energy levels in the cavity (Bohm, 1951). A characteristic quasimode wave function is depicted at the bottom.

Here the dimensionless Q factor characterizes the total losses in the resonator,

$$Q^{-1} = Q_{\text{diss}}^{-1} + Q_{\text{leak}}^{-1} \ll 1, \quad (2)$$

where Q_{diss} and Q_{leak} are the Q factors responsible for the dissipation and leakage, respectively. The dimensionless half-width of the resonant peak in the spectrum is given by

$$\delta\nu \equiv \frac{\delta\omega_{\text{res}}}{\omega_{\text{res}}} = Q^{-1}.$$

B. Plane wave interacting with a resonator

The tunneling of an incident plane wave through an open 1D resonator is characterized by the transmission and reflection coefficients T and R . The transmittance T

is usually small due to the opaque barriers, but if the frequency of the incident wave coincides with one of the eigenmode frequencies, an effective resonant tunneling occurs. The corresponding transmission coefficient T_{res} is given by (Bohm, 1951; Xu *et al.*, 2000; Bliokh *et al.*, 2006)

$$T_{\text{res}} = \frac{4Q_{\text{leak } 1}^{-1} Q_{\text{leak } 2}^{-1}}{(Q_{\text{leak } 1}^{-1} + Q_{\text{leak } 2}^{-1} + Q_{\text{diss}}^{-1})^2}. \quad (3)$$

Here $Q_{\text{leak } 1}$ and $Q_{\text{leak } 2}$ are the leakage Q factors ($Q_{\text{leak}}^{-1} = Q_{\text{leak } 1}^{-1} + Q_{\text{leak } 2}^{-1}$), which are related to the transmittances T_1 and T_2 of the two barriers by (Bliokh *et al.*, 2005)

$$Q_{\text{leak } 1,2}^{-1} = \frac{v_g T_{1,2}}{2\ell\omega_{\text{res}}}. \quad (4)$$

Here v_g is the wave group velocity inside the resonator and ℓ is the resonator cavity length (so that $2\ell/v_g$ is the round-trip travel time of the wave inside the cavity). Hereafter, we assume $\omega_{\text{res}}/v_g = k$, where k is the wave number of the resonant wave. Note that total transparency, $T_{\text{res}} = 1$, is achieved only in a dissipationless symmetric resonator, i.e.,

$$T_{\text{res}} = 1 \quad \text{when } Q_{\text{diss}}^{-1} = 0, \quad Q_{\text{leak } 1}^{-1} = Q_{\text{leak } 2}^{-1}. \quad (5)$$

The reflection coefficient R is close to unity off-resonance and is characterized by sharp resonant dips on-resonance. The resonant reflection coefficient is given by (Bohm, 1951; Xu *et al.*, 2000; Bliokh *et al.*, 2006)

$$R_{\text{res}} = \frac{(-Q_{\text{leak } 1}^{-1} + Q_{\text{leak } 2}^{-1} + Q_{\text{diss}}^{-1})^2}{(Q_{\text{leak } 1}^{-1} + Q_{\text{leak } 2}^{-1} + Q_{\text{diss}}^{-1})^2}. \quad (6)$$

In contrast to the transmittance (3), the reflectance (6) also reaches its minimum value in dissipative asymmetric resonators,

$$R_{\text{res}} = 0 \quad \text{when } Q_{\text{diss}}^{-1} = Q_{\text{leak } 1}^{-1} - Q_{\text{leak } 2}^{-1}. \quad (7)$$

This is the so-called *critical coupling* effect (Xu *et al.*, 2000). In the important particular case when the second barrier is opaque, $Q_{\text{leak } 2}^{-1} = 0$, $Q_{\text{leak } 1}^{-1} = Q_{\text{leak}}^{-1}$, so that the total transmittance vanishes, $T = 0$, the reflectance spectrum exhibits pronounced resonant dips, with $R_{\text{res}} = 0$, if the leakage and dissipation Q factors are equal to each other (see, e.g., Slater, 1950): $Q_{\text{diss}}^{-1} = Q_{\text{leak}}^{-1}$. Then, the incident wave is totally absorbed by an open resonator, so that all the wave energy penetrates into the resonator and dissipates therein.

C. Coupled resonators

Two resonators can be coupled by the fields penetrating through the barriers. This system (outside the critical-coupling regime) can be effectively described by the coupled oscillators model. When the first (incoming) resonator is excited by a monochromatic source with frequency ω , the appropriate oscillator equations can be written as follows:

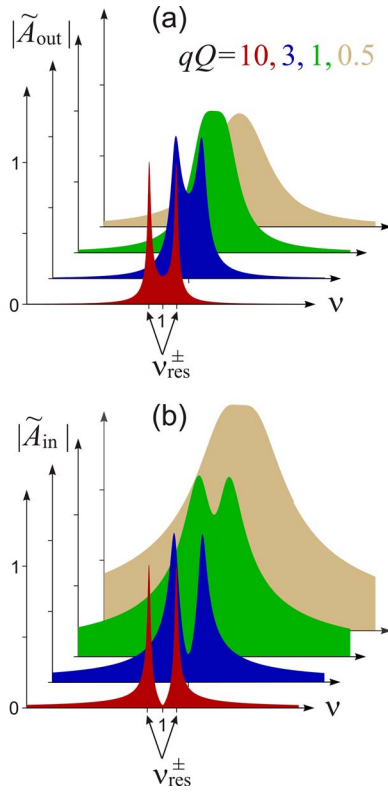


FIG. 6. (Color online) Near-resonant transmission of an incident wave through two coupled open resonators at different values of qQ . The normalized (i.e., multiplied by the factor $2Q^{-1}$) absolute values of the field amplitudes in two resonators, (a) $|\tilde{A}_{\text{out}}|$ and (b) $|\tilde{A}_{\text{in}}|$, are shown. In the dissipationless case ($Q_{\text{diss}}^{-1}=0$, $Q=Q_{\text{leak}}$), the transmission coefficient of the system is given by $T=|\tilde{A}_{\text{out}}|^2$.

$$\begin{aligned} \frac{d^2\psi_{\text{in}}}{d\tau^2} + Q^{-1}\frac{d\psi_{\text{in}}}{d\tau} + \psi_{\text{in}} &= q\psi_{\text{out}} + f_0e^{-i\nu\tau}, \\ \frac{d^2\psi_{\text{out}}}{d\tau^2} + Q^{-1}\frac{d\psi_{\text{out}}}{d\tau} + \psi_{\text{out}} &= q\psi_{\text{in}}, \end{aligned} \quad (8)$$

where ψ_{in} (ψ_{out}) is the field in the first (second) resonator, $\tau = \omega_{\text{res}}t$ and $\nu = \omega/\omega_{\text{res}}$ are the dimensionless time and frequency, $q \ll 1$ is the coupling coefficient, and f_0 is the effective exciting force from the incident field. The steady-state solutions of Eqs. (8) are oscillations with amplitudes A_{in} and A_{out} given by

$$\begin{aligned} A_{\text{in}} &= \frac{f_0(1 - \nu^2 - i\nu Q^{-1})}{(1 - \nu^2 - i\nu Q^{-1})^2 - q^2}, \\ A_{\text{out}} &= \frac{f_0q}{(1 - \nu^2 - i\nu Q^{-1})^2 - q^2}. \end{aligned} \quad (9)$$

Near resonance, $|\nu-1| \ll 1$, the frequency dependencies of these amplitudes at different values of the qQ factor are shown in Fig. 6. In the figure it can be seen that when the condition $qQ > 1$ is satisfied, there are two collective resonant modes with equal field amplitudes in

the two resonators. Their frequencies are shifted from the eigenfrequency of the oscillators, $\nu=1$, due to losses and coupling,

$$\nu_{\text{res}}^{\pm} = 1 \pm \frac{1}{2}\sqrt{q^2 - Q^{-2}}. \quad (10)$$

As qQ decreases, the resonant peaks in the spectra are located near each other and meet when $qQ=1$. In the regime $qQ < 1$, there is one peak at $\nu=1$.

The parameter qQ that appears in the model has a simple physical meaning: it determines whether the two resonators should be considered as essentially coupled or isolated. When $Q^{-1} \ll q$, the losses are negligible and the field characteristics are determined by the coupling. Remarkably, in this case the field intensity in the first (incoming) resonator is negligible at $\nu=1$, and most of the energy is concentrated in the second resonator: $A_{\text{out}} \gg A_{\text{in}}$. On the contrary, when the losses prevail over the coupling, $Q^{-1} \gg q$, the incident wave only excites the first resonator, and the energy is concentrated mostly in that resonator: $A_{\text{in}} \gg A_{\text{out}}$.

III. SURFACE PLASMON-POLARITON SYSTEMS

A. Basic features

The interface between materials with different signs of the permittivity, $\varepsilon > 0$ and $\varepsilon < 0$ (or permeability, $\mu > 0$ and $\mu < 0$), supports surface p - (or s -) polarized waves, also known as plasmon polaritons (PP). PP were discovered in 1957 by [Ritche \(1957\)](#) while studying a metal-vacuum interface. Renewed interest in plasmon polaritons comes from their considerable role in contemporary nanophysics ([Barnes *et al.*, 2003](#); [Zayats *et al.*, 2005](#)). The interface between regular ($\varepsilon > 0$, $\mu > 0$) and left-handed ($\varepsilon < 0$, $\mu < 0$) materials supports PP with an arbitrary polarization ([Ruppin, 2000](#)).

Plasmon polaritons are electromagnetic waves that are trapped at the interface, their electromagnetic fields decaying exponentially deep into both media [Fig. 7(a)]. Hence, the interface forms a peculiar resonator with eigenmodes that are localized along the normal to the interface but can propagate freely along the interface. Spatial eigenfunctions of this resonator have the form

$$\chi(\mathbf{r}) = \exp(-\kappa_z|z|)\exp(i\mathbf{k}_{\perp} \cdot \mathbf{r}_{\perp})$$

¹All these properties can be easily seen in our animated simulations at <http://dml.riken.jp/resonators/resonators.swf> where three regimes mimicking perfect lenses, enhanced transparency, and weak coupling (see Sec. III) are given.

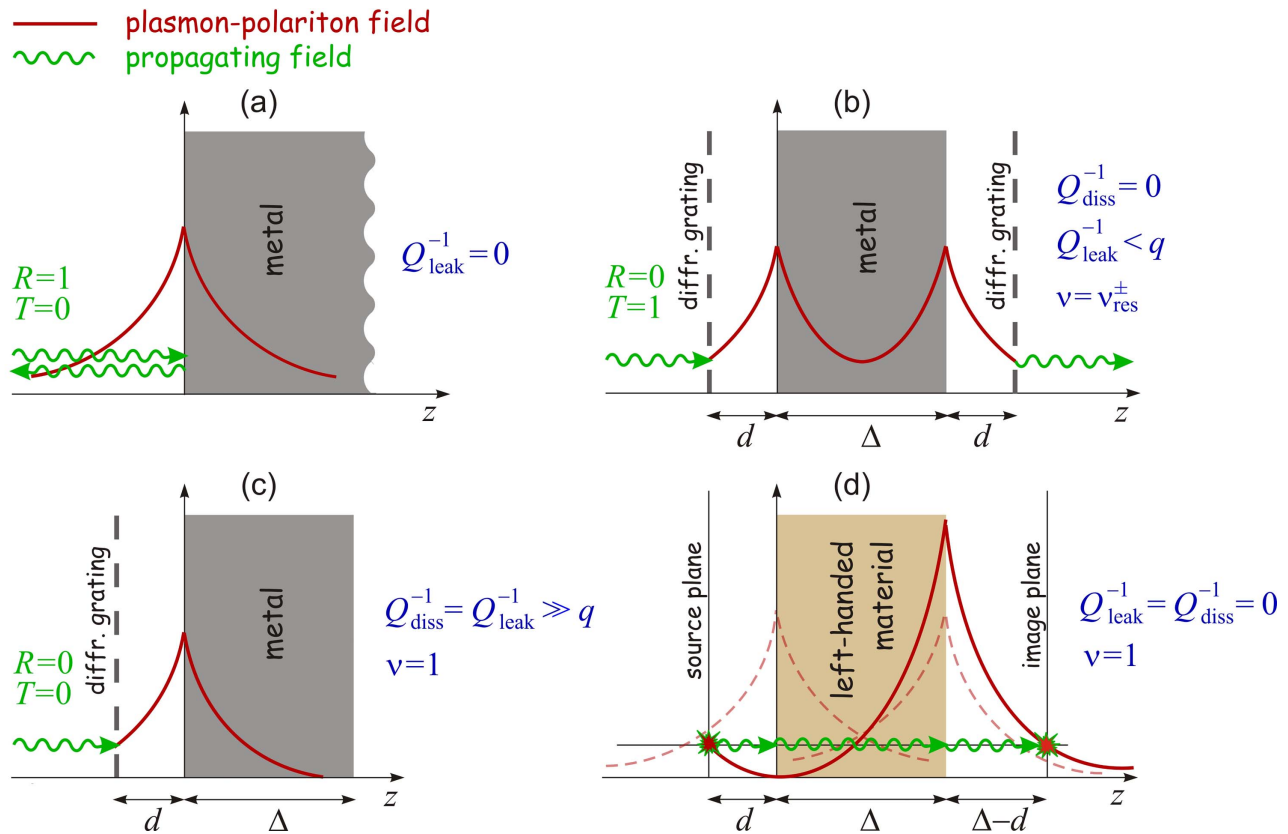


FIG. 7. (Color online) Schematic diagrams of surface plasmon-polariton (PP) resonators, their interaction with incident waves, and the corresponding resonator parameters. (a) A vacuum/metal interface supports plasmon modes localized in the z direction and the corresponding resonator parameters. Propagating and evanescent waves do not interact with each other, and, therefore, there is no energy leakage from the PP resonator. (b) A metal film represents a system of two PP resonators coupled by their fields. A diffraction grating [or total internal reflection (TIR) interface, Fig. 3] can transform a propagating wave into an evanescent wave and vice versa, thereby making the PP resonators open, $Q_{\text{leak}}^{-1} \neq 0$. Resonant total transparency can be achieved when the dissipation is negligible, whereas the coupling is strong enough; cf. Figs. 2 and 6. (c) In the critical-coupling regime, all of the incident wave is absorbed by the metal or plasma due to intrinsic dissipation, cf. Fig. 3. (d) A slab of an ideal LHM also represents two coupled PP resonators. There are two essential distinctions as compared to metal films: (i) A LHM is transparent for propagating fields and (ii) plasmon polaritons are always in resonance with evanescent fields from the source. The latter means that the PP field distribution corresponds to the $\nu=1$ point in Fig. 6, and the evanescent field energy is concentrated at the output surface in the dissipationless case. As a result, both propagating and evanescent fields form an exact copy of the source field in the focal point; cf. Fig. 1.

and are characterized by a dispersion relation $\mathbf{k}_{\perp} = \mathbf{k}_{\perp}^{\text{PP}}(\omega)$. Here the interface is associated with the $z=0$ plane, the subscript \perp indicates vectors within the (x, y) plane, and the decay constant κ_z can take different values in the two media. The plasmon-polariton resonator possesses all features that are inherent to usual resonators: eigenfrequency, Q factor, topography of eigenmode fields, etc. It will be shown below that the identification of PP as a resonator is more than an analogy, since it captures the main physical process underlying this phenomenon.

An exponential profile of the PP field suggests that it can interact with *evanescent*, nonpropagating fields from an external source, which are characterized by a purely imaginary wave-vector component: $k_z = \pm i\kappa_z$. Furthermore, an incident *propagating* electromagnetic plane wave cannot excite the PP resonator, because for propagating waves (PW) $k_{\perp}^{\text{PW}} < \omega/c$, whereas for plasmon polaritons $k_{\perp}^{\text{PP}} > \omega/c$. At the same time, evanescent waves

(EW) are characterized by $k_{\perp}^{\text{EW}} > \omega/c$ and can excite the PP resonator. There are methods to convert a propagating wave into an evanescent one. This allows the interaction of light with plasmon polaritons, which has led to a new branch of physics: *plasmonics* (see, e.g., Zayats et al., 2005; Ozbay, 2006; Maier, 2007).

B. Enhanced transparency of a metal film

Examine the transmission of a plane wave through an optically thick metal film perforated with small subwavelength holes, as shown in Fig. 2. Two surfaces of the smooth metal film can be associated with two identical PP resonators, coupled by their fields, as shown in Fig. 7(b). As has been observed, PPs cannot be directly excited by the incident plane wave; however, PPs can interact through periodic modulations of the surface (Tan et al., 2000; Bonod et al., 2003; Darmanyan and Zayats, 2003; Dykhne et al., 2003). The effective interaction of

PPs with light occurs at some resonance frequency $\omega = \omega_{\text{res}}$ (or angle of propagation $\alpha = \alpha_{\text{res}}$), at which their wave vectors differ by a reciprocal-lattice-vector \mathbf{K} ,

$$\mathbf{k}_{\perp}^{\text{PP}}(\omega_{\text{res}}) - \mathbf{k}_{\perp}^{\text{PW}}(\omega_{\text{res}}) = \mathbf{K}. \quad (11)$$

One can say that the PP wave vector shifted by a reciprocal-lattice vector acquires a real z component, or vice versa, the shifted propagating mode becomes evanescent in the z direction. Thus, the periodic structure can be considered as a *mode transformer*. (It is worth remarking that while in microwave electronics such structures are used for slowing down the eigenmodes, here we deal with a speedup of the PP eigenmodes.) The periodic corrugation of the metal surface can be treated as a diffraction grating placed on the surface. The grating can be located at a distance d from the smooth surface; it remains coupled with plasmons polaritons by their field (Bliokh, 2006; Lin *et al.*, 2006), as shown in Figs. 7(b) and 7(c).

Now we make use of the general theory of resonators. Assuming the dissipation to be negligible, $Q_{\text{diss}}=0$, the Q factor of the PP resonator is determined by the energy leakage from the resonator due to the transformation of the evanescent waves into the propagating ones,

$$Q_{\text{leak}}^{-1} = \gamma \exp(-2\kappa_z d). \quad (12)$$

Here $\gamma \ll 1$ is the transformation coefficient at the diffraction grating, and the exponential dependence arises due to decay of the evanescent field intensity between the metal surface and grating. The coupling coefficient between the two PP resonators is determined by the field of the first resonator acting on the second one,

$$q = \exp(-\kappa_z \Delta), \quad (13)$$

where Δ is the film thickness. The dependence of the transmission coefficient T on the normalized incident wave frequency ν is described by Eqs. (8)–(10), and is illustrated in Fig. 6(a). It exhibits two nearby peaks: $T_{\text{res}}=1$ at $\nu = \nu_{\text{res}}^{\pm}$ when $Q_{\text{leak}}^{-1} < q$, or one peak $T_{\text{res}} < 1$ at $\nu=1$ when $Q_{\text{leak}}^{-1} > q$. A characteristic field distribution for the total transmission is shown in Fig. 7(b). The coupling parameter decreases as Δ grows, and the transmission spectrum $T(\nu)$ changes as in Fig. 6(a). The same dependence of the transmission spectrum on the film thickness has been obtained by Tan *et al.* (2000), Martín-Moreno *et al.* (2001), Dykhne *et al.* (2003), Benabbas *et al.* (2005), and by many others concerned with particular geometries and specific modifications. In fact, all these features are general properties of two coupled resonators, independent of details.

Thus, light transmission through a perforated (corrugated) metal film can be divided into three processes: (i) transformation of the incident plane wave into an evanescent wave on the first diffraction grating, (ii) resonant “penetration” of the evanescent field through two coupled plasmon-polariton resonators, and (iii) reverse transformation into the propagating wave on the second grating, Fig. 7(b). It may seem at first that the larger the transformation coefficient at the diffraction grating, the

better is the transmission. However, larger transformation coefficients result in smaller Q factors. When γ exceeds a critical value, the transmission becomes less than 1 and decreases with γ (Dykhne *et al.*, 2003).

C. Critical coupling in optics and plasma physics

In the above model, it is easy to incorporate dissipation characterized by a small imaginary part of the dielectric constant, $\varepsilon = \varepsilon' + i\varepsilon''$, by introducing the dissipation Q factor,

$$Q_{\text{diss}}^{-1} = \frac{\varepsilon''}{|\varepsilon'|} \ll 1. \quad (14)$$

The dissipation is negligible only if $Q_{\text{diss}}^{-1} \ll \min(Q_{\text{leak}}^{-1}, q)$. Otherwise, even very small dissipation will drastically affect the resonance phenomena as it is compared to the exponentially small parameters (12) and (13). If $Q_{\text{diss}}^{-1} \sim Q_{\text{leak}}^{-1}$, dissipation may substantially suppress the transmission. When $Q_{\text{diss}}^{-1} \geq q$, dissipation breaks down the coupling between two PP resonators on either side of the film, and they can be regarded as essentially independent. For the system under consideration, this means that only the first resonator will be excited by the incident wave and the metallic film can be considered as a semi-infinite medium, Fig. 7(c). In such a case, transmission through the film vanishes at all frequencies. At the same time, the resonances show up in the reflection spectrum, which exhibits sharp dips at some frequencies. For some critical distance between the diffraction grating and metal, $d=d_c$, the resonant reflectance drops to zero, $R_{\text{res}}=0$, and the incident wave is totally absorbed by the metal, Fig. 3. This effect can be explained in terms of the same resonator model: (i) the incident plane wave transforms into an evanescent mode at the diffraction grating and (ii) the incident wave excites a PP resonator at the metal surface and is totally absorbed due to the critical coupling effect, Fig. 7(c). In our case, the critical coupling condition, Eq. (7), reads $Q_{\text{diss}}^{-1} = Q_{\text{leak}}^{-1}$ with Eqs. (12) and (14). Application of diffraction gratings for the PP resonator excitation is convenient in plasma experiments. When a properly designed grating is placed in front of the plasma surface, the reflected wave vanishes; see Fig. 3, bottom (Bliokh *et al.*, 2005; Wang *et al.*, 2006).

An analogous phenomenon in optics is known as frustrated total internal reflection (Otto, 1968). Similar to a diffraction grating, a total internal reflection interface can be used for plasmon-polariton excitation on a metal surface (Kretschmann and Raether, 1968; Otto, 1968). In the so-called Otto configuration, a metal is placed a distance d from the bottom of a prism where light is totally reflected (top of Fig. 3). The incident light, with $k_{\perp}^{\text{PW}} < \omega/c$, penetrates into the prism with the wave-vector projection $nk_{\perp}^{\text{PW}} > \omega/c$ ($n > 1$ is the refractive index of the prism). The incident light generates an evanescent wave in vacuum near the bottom and can excite the PP resonator at a resonance frequency $\omega = \omega_{\text{res}}$ (or angle of propagation $\alpha = \alpha_{\text{res}}$), where

$$\mathbf{k}_\perp^{\text{PP}} = n\mathbf{k}_\perp^{\text{PW}}. \quad (15)$$

The leakage Q factor of the PP resonator is given by Eq. (12), where $\gamma \sim 1$ is the coefficient of transformation to the evanescent wave at the bottom of the prism. At a critical distance $d = d_c$, the reflected light disappears, which provides evidence of the critical-coupling regime. Note that when the metal film is so thin that $q \geq Q^{-1}$, the high resonant transparency of the film can be observed when the identical prism is located symmetrically near the opposite side of the film (Dragila *et al.*, 1985). This configuration is analogous to the above-considered grating-metal-grating system, Fig. 7(b).

Total absorption of an incident wave due to the critical coupling can be used for the simultaneous determination of both the real and imaginary parts of the metal (plasma) permittivity. On the one hand, the resonant frequency ω_{res} (or the angle of incidence) is determined by the resonance with the PP mode, which depends on the real part of the metal permittivity ε' . On the other hand, the critical-coupling distance d_c between the prism (grating) and the metal (plasma) surface depends on the dissipative Q factor (14) related to the imaginary part ε'' of the permittivity. Thus, the critical-coupling regime provides a mapping between $(\omega_{\text{res}}, d_c)$ and $(\varepsilon', \varepsilon'')$ and makes it possible to retrieve the complex permittivity of the metal (plasma) via external measurements.

D. Super-resolution of LHM lenses

While a dielectric medium is transparent for propagating plane waves and a metal surface supports PP evanescent modes, a left-handed material combines both of these features. Let the source of a monochromatic electromagnetic field (the object) be located at a distance d from the surface of a flat slab of an “ideal” LHM ($\varepsilon = \mu = -1$) of width $\Delta > d$, as shown in Fig. 7(d). The source radiates propagating plane-wave harmonics with $k_\perp^{\text{PW}} \leq \omega/c$, as well as evanescent waves with

$$k_\perp^{\text{EW}} > \frac{\omega}{c}. \quad (16)$$

The propagating waves are focused by the LHM slab and form the image on the opposite side of the slab, Fig. 1. The ideal LHM is perfectly matched with the vacuum due to the equivalence of their impedances $Z = \sqrt{\mu/\varepsilon}$, and, therefore, there is no reflected wave in this case. The image field is almost equal to the source one: all plane waves reach the focal plane (located at a distance $\Delta - d$ from the slab) with the same phase as they had in the source plane. The aberration (imperfection) of the image might only be caused by the loss of evanescent harmonics, which are responsible for the subwavelength details of the object.

Remarkably, even subwavelength information is not lost in the ideal LHM (Pendry’s) lens. This can be understood if we consider the surfaces of the LHM slab as two coupled PP resonators, as done to explain the high transmission of the perforated metallic films. Evanescent

waves from the source excite the first PP resonator. A distinguishing feature of the PP mode at the ideal LHM/vacuum interface is that its dispersion relation is precisely the same as for evanescent modes in the vacuum (Ruppin, 2000). This implies that *all* evanescent waves (16) are in resonance with the PP resonator on the ideal LHM surface (Haldane, 2002). In other words, $\omega \equiv \omega_{\text{res}}$ and $\nu \equiv 1$ for any frequency (the material dispersion is neglected here).

The evanescent field distribution can be found from Eqs. (8) and (9). The PP resonators at the dissipationless LHM surface are characterized by an infinite Q factor,

$$Q_{\text{leak}}^{-1} = 0, \quad (17)$$

because there is no leakage from the PP to radiative modes. We associate the amplitudes A_{in} and A_{out} with the field amplitude at the input and output surfaces of the slab. Then the effective external force is given by

$$f_0 = A_0 \exp(-\kappa_z d),$$

where A_0 is the amplitude of the evanescent field of the source. The coupling parameter is given by Eq. (13), the same as for the metallic film. According to Eqs. (9) with $\nu = 1$ and $Q^{-1} = 0$ (see also Fig. 6), the input resonator is not excited,

$$|A_{\text{in}}| = 0,$$

whereas the amplitude at the output is exponentially large,

$$|A_{\text{out}}| = \frac{|f_0|}{q} = |A_0| \exp[-\kappa_z(d - \Delta)].$$

In the image half-space, the evanescent field decreases with the same decrement κ_z , and at the distance $\Delta - d$ from the second interface (the total distance from the source is 2Δ) it takes on the initial value [Fig. 7(d)]

$$|A(2\Delta)| = |A_0|.$$

Since the phases of evanescent waves are not changed along the z axis, the evanescent fields in the focal plane precisely reproduce those in the source plane. This means that the image created by both propagating and evanescent waves is a *perfect* copy of the source. Exactly the same evanescent field distribution in Pendry’s lens follows from the accurate solution of the Maxwell equations (see, e.g., Haldane, 2002; Gómez-Santos, 2003). It is worth noting that the electromagnetic nature of waves has not been involved in our consideration of subwavelength imaging. The same result can be achieved using other kinds of waves, for example, liquid-surface waves (Hu *et al.*, 2004), surface electromagnetic waves propagating along special types of interfaces (Shadrivov *et al.*, 2004; Kats *et al.*, 2007), and surface Josephson plasma waves (Savel’ev *et al.*, 2005) in layered superconductors.

If a small dissipation is present in LHM, it can be taken into account by introducing the dissipation Q factor (14) in Eqs. (8) and (9) (here, for simplicity, the permeability is assumed to be real). The destructive effect of dissipation in the LHM, reducing the image quality, is

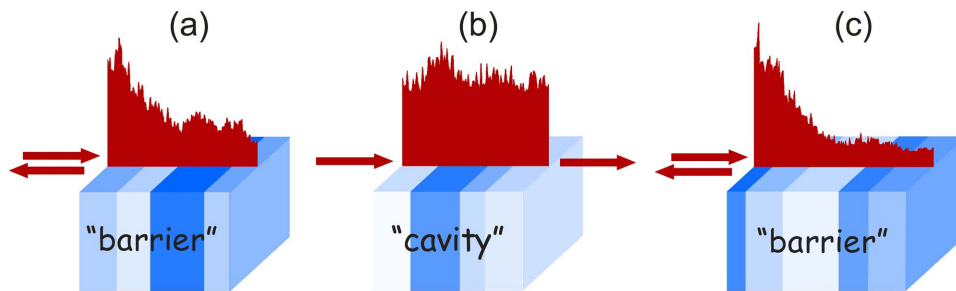


FIG. 8. (Color online) The sample in Fig. 4 is now “cut” into three separate segments that are considered independently. It can be seen that while the right- and left-side segments are practically opaque due to Anderson localization, the central part (where a large energy concentration has been observed in resonance) happens to be almost transparent for the resonant frequency. This provides the standard barrier-cavity-barrier resonator structure, which explains the resonant features of the sample at a given frequency.

defined by the ratio between the Q factor and the coupling parameter q . When $Q_{\text{diss}}^{-1} \ll q$, the image aberration is small. When $Q_{\text{diss}}^{-1} \geq q = \exp(-\kappa_z \Delta)$, the dissipation is crucial and practically destroys the penetration of evanescent waves through the LHM slab. This limitation of the ideality of Pendry’s lens has been discussed by Garcia and Nieto-Vesperinas (2002), and Nieto-Vesperinas (2004) using a wave approach. At the same time, the dissipation affects the propagating waves in a LHM lens in the same manner as in normal media, because the LHM slab does not form a resonator for propagating waves. The dissipation significantly affects the propagation waves only when $Q_{\text{diss}}^{-1} \geq (k\Delta)^{-1} \gg q$.

IV. RANDOM MEDIA

A. Resonant tunneling

The resonant transmission of waves through a 1D random sample is accompanied by a large concentration of energy inside the sample, as shown in Fig. 4. Such field distributions can be regarded as quasimodes of an open system. Among various localized states, high transparency accompanies only those modes that are located near the center of the sample. Localized modes and anomalous transparency can be explained by the existence of effective high- Q resonator cavities inside of the sample. Figure 8 demonstrates the transparencies of different parts of the sample from Fig. 4. It is clearly seen that the middle section, where the energy was concentrated, is almost transparent to the resonant frequencies, while the side parts are practically opaque to the wave. Thus, each localized state at a frequency $\omega = \omega_{\text{res}}$ can be associated with a typical resonator structure comprised of an almost transparent segment (“cavity”) bounded by essentially nontransparent regions (“barriers”) (Bliokh *et al.*, 2004). Wave tunneling through such a system can be treated as a particular case for the general problem of the transmission through an open resonator. The distinguishing feature of the random medium is that there are no regular walls (the medium is locally transparent in each point) and transmittances of barriers are exponentially small as a result of Anderson localization. More-

over, different segments of the sample turn out to be transparent for different frequencies, i.e., each localized mode is associated with its own resonator.

The resonant tunneling through a random sample can be described by Eq. (3), where the barrier transmittances and Q factors are estimated as (Bliokh *et al.*, 2004)

$$T_{1,2} \approx \exp\left(-\frac{2L_{1,2}}{\ell_{\text{loc}}}\right), \quad Q_{\text{leak } 1,2}^{-1} = \frac{T_{1,2}}{2k\ell}, \quad (18)$$

and the total leakage Q factor is $Q_{\text{leak}}^{-1} = Q_{\text{leak } 1}^{-1} + Q_{\text{leak } 2}^{-1}$. Here L_1 and L_2 are the distances from the cavity to the ends of the sample (the barrier lengths) and ℓ_{loc} is the localization length. The latter is the only spatial scale responsible for the localization, and the cavity size should be estimated as $\ell \sim \ell_{\text{loc}}$. This simple model drastically reduces the level of complexity of the problem: the disordered medium with a large number of random elements can be effectively described now through a few characteristic scales, namely the localization length, the wavelength, and the size of the sample. All the main features and characteristics of the resonances (transmittance, field intensity, spectral half-width, and the density of states) can be estimated from the resonator model, in good agreement with experimental data (Bliokh *et al.*, 2006). In particular, the perfect resonant transmission takes place only for a symmetric dissipationless resonator, Eq. (5), which corresponds to wave localization in the middle of the sample and a maximal total Q factor.

Note that a long enough sample can contain two or more isolated transparent regions where the wave field is localized. These form the so-called “necklace states” predicted by Lifshits and Kirpichenkov (1979) and Pendry (1987) and observed by Bertolotti *et al.* (2005) and Sebbah *et al.* (2006). Necklace states can be easily incorporated in our general scheme as two or more resonators coupled by their evanescent fields, Eqs. (8)–(10) (Bliokh *et al.*, 2008). The coupling coefficient between the nearest resonators is

$$q \approx \exp\left(-\frac{\Delta}{\ell_{\text{loc}}}\right), \quad (19)$$

where Δ is the distance between the effective cavities.

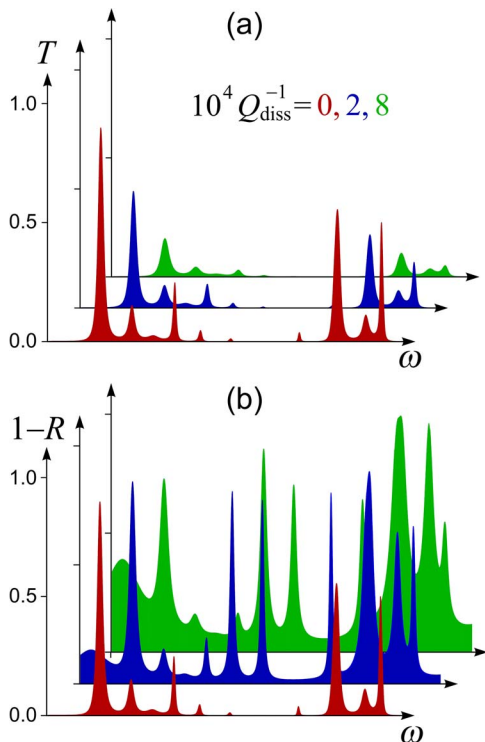


FIG. 9. (Color online) Spectra of (a) the transmittance T and (b) the reflectance R for various values of the dissipation rate Q_{diss} in a random dielectric sample. Although the dissipation is extremely small, peaks of resonant transmittance disappear rapidly when the dissipation increases. At the same time, peaks in $1-R$ become sharply pronounced and become even more informative than in the dissipationless case. Resonances with $R=T=0$ evidence the critical-coupling regime.

B. Critical coupling

It seems reasonable to assume that dissipation in the sample material worsens the observability of resonances. However, surprisingly, small losses can improve the conditions for the detection of localized states. A large number of resonances, which are not visible in the transmission spectrum, become easily detected in the *reflection* spectrum (Bliokh *et al.*, 2006), Fig. 9. This is clarified in terms of the critical-coupling phenomenon. If the dissipation Q_{diss}^{-1} , given by Eq. (14), exceeds the leakage Q_{leak}^{-1} for modes localized in the middle of the sample,

$$Q_{\text{diss}}^{-1} > \frac{1}{k\ell_{\text{loc}}} \exp\left(-\frac{L}{\ell_{\text{loc}}}\right),$$

the transmission is strongly suppressed for all frequencies, and $T \ll 1$. At the same time, the other states located closer to the input of the sample and, therefore, characterized by higher Q_{leak}^{-1} can be excited. According to the critical-coupling condition (7), the resonant reflectance drops to zero when the dissipation and leakage Q factors are of the same order. For modes localized in the first half of the sample, we can set, with exponential accuracy, $Q_{\text{leak } 2}^{-1} \approx 0$, $Q_{\text{leak } 1}^{-1} = Q_{\text{leak}}^{-1}$, so that the critical-coupling condition reads $Q_{\text{diss}}^{-1} = Q_{\text{leak}}^{-1}$ for the case of a semi-infinite medium.

The resonator model enables one to find characteristic parameters of localized states and the sample via external measurements of the transmission and reflection coefficients (Bliokh *et al.*, 2004, 2006; Scales *et al.*, 2007). By measuring resonant and typical off-resonance values of the transmittance and reflectance, Eqs. (3) and (6), along with the resonance spectral half-width, it is possible to determine (at least to estimate) the localization length, dissipation factor, position of the localized state, and its field intensity. Some of these internal quantities usually cannot be determined via direct measurements, but are crucial, for example, for the random lasing problem. For instance, the critical-coupling condition connects the position of the localization region with the dissipation rate in the medium, while the latter can be determined through the half-width of the resonant deep in the reflectance.

It should also be noted that random systems consisting of repeated elements of several types can exhibit transmission resonances of another kind, which are not accompanied by the energy localization and cannot be described by the resonator model (see, e.g., Hendricks and Teller, 1942; Tamura and Nori, 1989, 1990; Kolar *et al.*, 1991; Nishiguchi *et al.*, 1993a, 1993b).

V. CONCLUDING REMARKS

The subwavelength resolution of a flat LHM lens, abnormal transparency of a perforated metal film, localized states in disordered media, frustrated total internal reflection, and total absorption of an electromagnetic wave by an overdense plasma are all phenomena related to different areas of physics and are characterized by different spatial scales, from the nanoscale to centimeters and larger. In spite of such enormous differences, the main properties of these phenomena have much in common with each other and, on a deeper level, with simple resonator systems. As we have shown, all these phenomena can be treated in a universal way as wave transmission through one or two coupled resonators. A careful mapping between the resonator and the problem parameters allows one to understand thoroughly the physical properties of the problem and forecast how the parameters affect the result.

Of course, accurate descriptions of wave transmission through complex systems (for example, periodically perforated metal films or random media) involve particular details of a given sample and depend on the geometry of the periodic structure or the specific realization of the random process. Nonetheless, fundamental features of these systems that are independent of details can be revealed only through a unified approach emphasizing the physical essence of the problem. Resonator models provide such an approach. In some cases (e.g., for evanescent fields in the LHM lens), resonator description results in the *exact* solution of the problem. Furthermore, in the case of random media, such a model is the *only* formalism that enables one to estimate the parameters of the individual localized states.

One of the important common features of all resona-

TABLE I. Mapping between the classical resonator characteristics and parameters of various physical systems discussed in this work.

Resonator characteristics	Enhanced transparency	Total absorption in plasma	Frustrated TIR in optics	Ideal LHM lens	Localization in random medium
Dissipation Q factor Q_{diss}^{-1}	$\varepsilon''/ \varepsilon' $				
Leakage Q factor Q_{leak}^{-1}	$\gamma \exp(-2\kappa_z d)$			0	$(T_1 + T_2)/2k\ell_{\text{loc}}$, $T_{1,2} = \exp(-2L_{1,2}/\ell_{\text{loc}})$
Coupling coefficient q	$\exp(-\kappa_z \Delta)$			$\exp(-\kappa_z \Delta)$	$\exp(-\Delta/\ell_{\text{loc}})$
Resonance condition $\omega = \omega_{\text{res}}$	$\mathbf{k}_{\perp}^{\text{PP}} - \mathbf{k}_{\perp}^{\text{PW}} = \mathbf{K}$		$\mathbf{k}_{\perp}^{\text{PP}} = n\mathbf{k}_{\perp}^{\text{PW}}$	$k_{\perp}^{\text{EW}} > \omega/c$	$\omega = \omega_{\text{res}}$

tor systems is their high sensitivity to internal dissipation. Even very small dissipation, which has negligible effects for propagating waves, may drastically modify the localized resonance states. Usually dissipation destroys the resonant transmission but develops resonant dips in the reflection spectrum. The reason for this is that the excitation of a resonator is always accompanied by a huge field intensity therein, proportional to the Q factor. The energy dissipated per unit time is determined by the product of the dissipation rate and the field intensity. Thus, a small dissipation rate is multiplied by a high Q factor and can be crucial. Also, establishing a one-to-one correspondence with classical resonator allows us to retrieve the *internal* characteristics of an investigated system using the *external* response to a probing signal (incident wave). In this way, one can determine the complex permittivity of metal or plasma, location and field intensity of localized states in random medium, etc. Remarkably, dissipation can be favorable for such purposes, revealing some hidden internal features through the critical-coupling effect.

To conclude, the central result of this colloquium, i.e., the mapping between the resonator and the problems' parameters, is summarized in Table I. We have considered only a few, probably more intriguing and nontrivial, systems allowing the resonator consideration. A more complete list of such systems would be much longer, since any wave system with localized modes can be treated as a generalized resonator. In particular, numerous quantum systems (not considered here) with potential wells, tunneling, and relaxation could be effectively treated within the open-resonator framework (see, e.g., You and Nori, 2005; Lazarides and Tsironis, 2007; Rakhmanov *et al.*, 2007; Savel'ev *et al.*, 2007). Finally, it should also be noted that for some of the systems considered above, there exist alternative *ad hoc* methods of description. For instance, negative refraction and optical cloaking allow a natural representation in the geometrical formalism of general relativity (Leonhardt and Philbin, 2006).

ACKNOWLEDGMENTS

F.N. gratefully acknowledges partial support from the National Security Agency (NSA), Laboratory Physical Science (LPS), Army Research Office (ARO), and National Science Foundation (NSF) Grant No. EIA-0130383. F.N. and S.S. acknowledge partial support from JSPS-RFBR 06-02-91200 and the Core-to-Core (CTC) program supported by the Japan Society for the Promotion of Science (JSPS). K.Y.B. acknowledges support from STCU Grant No. P-307 and CRDF Grant No. UAM2-1672-KK-06. S.S. acknowledges support from the Ministry of Science, Culture and Sport of Japan via the Grant-in Aid for Young Scientists No. 18740224, the UK EPSRC via No. EP/D072581/1, No. EP/F005482/1, and the ESF network-programme "Arrays of Quantum Dots and Josephson Junctions."

REFERENCES

- Anderson, P. W., 1958, "Absence of diffusion in certain random lattices," *Phys. Rev.* **109**, 1492.
- Azbel, M. Y., 1983, "Eigenstates and properties of random systems in one dimension at zero temperature," *Phys. Rev. B* **28**, 4106.
- Azbel, M. Y., and P. Soven, 1983, "Transmission resonances and the localization length in one-dimensional disordered systems," *Phys. Rev. B* **27**, 831.
- Barnes, W. L., A. Dereux, and T. M. Ebbesen, 2003, "Surface plasmon subwavelength optics," *Nature* **424**, 824.
- Benabbas, A., V. Halté, and J.-Y. Bigot, 2005, "Analytical model of the optical response of periodically structured metallic films," *Opt. Express* **13**, 8730.
- Berry, M. V., and S. Klein, 1997, "Transparent mirrors: Rays, waves and localization," *Eur. J. Phys.* **18**, 222.
- Bertolotti, J., S. Gottardo, D. S. Wiersma, M. Ghulinyan, and L. Pavesi, 2005, "Optical necklace states in Anderson localized 1D systems," *Phys. Rev. Lett.* **94**, 113903.
- Bliokh, K. Y., and Y. P. Bliokh, 2004, "What are the left-handed media and what is interesting about them?," *Phys. Usp.* **47**, 393.
- Bliokh, K. Y., Y. P. Bliokh, and V. D. Freilikher, 2004, "Resonances in one-dimensional disordered systems: Localization

- of energy and resonant transmission,” *J. Opt. Soc. Am. B* **21**, 113.
- Bliokh, K. Y., Y. P. Bliokh, V. Freilikher, A. Z. Genack, B. Hu, and P. Sebbah, 2006, “Localized modes in open one-dimensional dissipative random systems,” *Phys. Rev. Lett.* **97**, 243904.
- Bliokh, K. Y., Y. P. Bliokh, V. Freilikher, A. Z. Genack, and P. Sebbah, 2008, “Coupling and level repulsion in the localized regime: From isolated to quasi-extended modes,” e-print arXiv:0806.0704, *Phys. Rev. Lett.* (to be published).
- Bliokh, Y. P., 2006, “Plasmon mechanism of light transmission through a metal film or a plasma layer,” *Opt. Commun.* **259**, 436.
- Bliokh, Y. P., J. Felsteiner, and Y. Z. Slutsker, 2005, “Total absorption of an electromagnetic wave by an overdense plasma,” *Phys. Rev. Lett.* **95**, 165003.
- Bohm, D., 1951, *Quantum Theory* (Prentice-Hall, New York).
- Bonod, N., S. Enoch, L. Li, E. Popov, and M. Neviere, 2003, “Resonant optical transmission through metallic films with and without holes,” *Opt. Express* **11**, 482.
- Cao, H., Y. G. Zhao, S. T. Ho, E. W. Seelig, Q. H. Wang, and R. P. H. Chang, 1999, “Random laser action in semiconductor powder,” *Phys. Rev. Lett.* **82**, 2278.
- Darmanyan, S. A., and A. V. Zayats, 2003, “Light tunneling via resonant surface plasmon polariton states and the enhanced transmission of periodically nanostructured metal films: An analytical study,” *Phys. Rev. B* **67**, 035424.
- Dragila, R., B. Luther-Davies, and S. Vukovic, 1985, “High transparency of classically opaque metallic films,” *Phys. Rev. Lett.* **55**, 1117.
- Dykhne, A. M., A. K. Sarychev, and V. M. Shalaev, 2003, “Resonant transmittance through metal films with fabricated and light-induced modulation,” *Phys. Rev. B* **67**, 195402.
- Ebbesen, T. W., H. J. Lezec, H. F. Ghaemi, T. Thio, and P. A. Wolff, 1998, “Extraordinary optical transmission through sub-wavelength hole arrays,” *Nature* **391**, 667.
- Eleftheriades, G. V., and K. G. Balman, 2005, *Negative-Refractive Metamaterials: Fundamental Principles and Applications* (Wiley, New York).
- Fang, N., H. Lee, C. Sun, and X. Zhang, 2005, “Sub-diffraction-limited optical imaging with a silver superlens,” *Science* **308**, 534.
- Freilikher, V. D., and S. A. Gredeskul, 1992, “Localization of waves in media with one-dimensional disorder,” *Prog. Opt.* **30**, 137.
- García, N., and M. Nieto-Vesperinas, 2002, “Left-handed materials do not make a perfect lens,” *Phys. Rev. Lett.* **88**, 207403.
- García de Abajo, F. J., 2007, “Light scattered by particle and hole arrays,” *Rev. Mod. Phys.* **79**, 1267.
- Genet, C., and T. W. Ebbesen, 2007, “Light in tiny holes,” *Nature* **445**, 39.
- Gómez-Santos, G., 2003, “Universal features of the time evolution of evanescent modes in a left-handed perfect lens,” *Phys. Rev. Lett.* **90**, 077401.
- Haldane, F. D. M., 2002, “Electromagnetic surface modes at interfaces with negative refractive index make a ‘not-quite-perfect’ lens,” e-print arXiv:cond-mat/0206420.
- Hendricks, S., and E. Teller, 1942, “X-ray interference in partially ordered layer lattices,” *J. Chem. Phys.* **10**, 147.
- Hu, X., Y. Shen, X. Liu, R. Fu, and J. Zi, 2004, “Superlensing effect in liquid surface waves,” *Phys. Rev. E* **69**, 030201(R).
- Kats, A. V., S. Savel’ev, V. A. Yampol’skii, and F. Nori, 2007, “Left-handed interfaces for electromagnetic surface waves,” *Phys. Rev. Lett.* **98**, 073901.
- Kolar, M., M. K. Ali, and F. Nori, 1991, “Generalized Thue-Morse chains and their properties,” *Phys. Rev. B* **43**, 1034.
- Kretschmann, E., and H. Raether, 1968, “Radiative decay of nonpropagating surface plasmons excited by light,” *Z. Naturforsch. A* **23**, 2135.
- Lazarides, N., and G. P. Tsironis, 2007, “rf superconducting quantum interference device metamaterials,” *Appl. Phys. Lett.* **90**, 163501.
- Leonhardt, U., and T. G. Philbin, 2006, “General relativity in electrical engineering,” *New J. Phys.* **8**, 247.
- Lezec, H. J., A. Degiron, E. Devaux, R. A. Linke, L. Martin-Moreno, F. J. García-Vidal, and T. W. Ebbesen, 2002, “Beaming light from a subwavelength aperture,” *Science* **297**, 820.
- Lifshits, I. M., S. A. Gredeskul, and L. A. Pastur, 1988, *Introduction to the Theory of Disordered Systems* (Wiley, New York).
- Lifshits, I. M., and V. Y. Kirpichenkov, 1979, “Tunnel transparency of disordered systems,” *Sov. Phys. JETP* **50**, 499.
- Lin, L., R. J. Reeves, and R. J. Blaikie, 2006, “Surface-plasmon-enhanced light transmission through planar metallic films,” *Phys. Rev. B* **74**, 155407.
- Maier, S. A., 2007, *Plasmonics: Fundamentals and Applications* (Springer, New York).
- Martín-Moreno, L., F. J. García-Vidal, H. J. Lezec, K. M. Pellerin, T. Thio, J. B. Pendry, and T. W. Ebbesen, 2001, “Theory of extraordinary optical transmission through subwavelength hole arrays,” *Phys. Rev. Lett.* **86**, 1114.
- Milner, V., and A. Z. Genack, 2005, “Photon localization laser: Low-threshold lasing in a random amplifying layered medium via wave localization,” *Phys. Rev. Lett.* **94**, 073901.
- Nieto-Vesperinas, M., 2004, “Problem of image super-resolution with a negative-refractive-index slab,” *J. Opt. Soc. Am. A* **21**, 491.
- Nishiguchi, N., S. I. Tamura, and F. Nori, 1993a, “Phonon transmission rate, fluctuations, and localization in random semiconductor superlattices: Green’s function approach,” *Phys. Rev. B* **48**, 2515.
- Nishiguchi, N., S. I. Tamura, and F. Nori, 1993b, “Phonon universal transmission fluctuations and localization in semiconductor superlattices with a controlled degree of order,” *Phys. Rev. B* **48**, 14426.
- Otto, A., 1968, “Excitation of nonradiative surface plasma waves in silver by the method of frustrated total reflection,” *Z. Phys.* **216**, 398.
- Ozbay, E., 2006, “Plasmonics: Merging photonics and electronics at nanoscale dimensions,” *Science* **311**, 189.
- Pendry, J. B., 1987, “Quasi-extended electron states in strongly disordered systems,” *J. Phys. C* **20**, 733.
- Pendry, J. B., 2000, “Negative refraction makes a perfect lens,” *Phys. Rev. Lett.* **85**, 3966.
- Rakhmanov, A. L., A. M. Zagoskin, S. Savel’ev, and F. Nori, 2007, “Quantum metamaterials: Electromagnetic waves in a Josephson qubit line,” e-print arXiv:0709.1314.
- Ritche, R. H., 1957, “Plasma losses by fast electrons in thin films,” *Phys. Rev.* **106**, 874.
- Ruppín, R., 2000, “Surface polaritons of a left-handed medium,” *Phys. Lett. A* **277**, 61.
- Sambles, R., 1998, “More than transparent,” *Nature* **391**, 641.
- Savel’ev, S., A. L. Rakhmanov, and F. Nori, 2007, “Quantum terahertz electrodynamics and macroscopic quantum tunneling in layered superconductors,” *Phys. Rev. Lett.* **98**, 077002.

- Savel'ev, S., V. Yampol'skii, and F. Nori, 2005, "Surface Josephson plasma waves in layered superconductors," *Phys. Rev. Lett.* **95**, 187002.
- Scales, J. A., L. D. Carr, D. B. McIntosh, V. Freilikher, and Y. P. Bliokh, 2007, "Millimeter wave localization: Slow light and enhanced absorption in random dielectric media," *Phys. Rev. B* **76**, 085118.
- Sebbah, P., B. Hu, J. M. Klosner, and A. Z. Genack, 2006, "Extended quasimodes within nominally localized random waveguides," *Phys. Rev. Lett.* **96**, 183902.
- Shadrivov, I. V., A. A. Sukhorukov, Y. S. Kivshar, A. A. Zharov, A. D. Boardman, and P. Egan, 2004, "Nonlinear surface waves in left-handed materials," *Phys. Rev. E* **69**, 016617.
- Shalaev, V. M., 2007, "Optical negative-index metamaterials," *Nat. Photonics* **1**, 41.
- Sheng, P., 1990, *Scattering and Localization of Classical Waves in Random Media* (World Scientific, Singapore).
- Slater, J. C., 1950, *Microwave Electronics* (Van Nostrand, Princeton).
- Smith, D. R., J. B. Pendry, and M. C. K. Wiltshire, 2004, "Metamaterials and negative refractive index," *Science* **305**, 788.
- Tamura, S., and F. Nori, 1989, "Transmission and frequency spectra of acoustic phonons in Thue-Morse superlattices," *Phys. Rev. B* **40**, 9790.
- Tamura, S. I., and F. Nori, 1990, "Acoustic interference in random superlattices," *Phys. Rev. B* **41**, 7941.
- Tan, W. C., T. W. Preist, and R. J. Sambles, 2000, "Resonant tunneling of light through thin metal films via strongly localized surface plasmons," *Phys. Rev. B* **62**, 11134.
- Veselago, V. G., 1967, "The electrodynamics of substances with simultaneously negative values of ϵ and μ ," *Usp. Fiz. Nauk* **92**, 517.
- Veselago, V. G., and E. E. Narimanov, 2006, "The left hand of brightness: Past, present and future of negative index materials," *Nat. Mater.* **5**, 759.
- Wang, Y., J.-X. Cao, G. Wang, L. Wang, Y. Zhu, and T.-Y. Niu, 2006, "Total absorption of electromagnetic radiation in overdense plasma," *Phys. Plasmas* **13**, 073301.
- Wiersma, D. S., 2000, "The smallest random laser," *Nature* **406**, 132.
- Xu, Y., Y. Li, R. K. Lee, and A. Yariv, 2000, "Scattering-theory analysis of waveguide-resonator coupling," *Phys. Rev. E* **62**, 7389.
- You, J. Q., and F. Nori, 2005, "Superconducting circuits and quantum information," *Phys. Today* **58** (11), 42.
- Zayats, A. W., I. I. Smolyaninov, and A. A. Maradudin, 2005, "Nano-optics of surface plasmon polaritons," *Phys. Rep.* **408**, 131.